Multinuclear nuclear magnetic resonance relaxation investigations of poly(propylene oxide) complexed with sodium trifluoromethanesulphonate

John P. Manning, Cheryl Baldwin Frech, B. M. Fung and Roger E. Frech*
Department of Chemistry and Biochemistry, University of Oklahoma, Norman, OK 73019-0370, USA
(Received 10 October 1990; accepted 19 October 1990)

Low molecular weight poly(propylene oxide), PPO, was complexed with varying amounts of sodium trifluoromethanesulphonate, $NaCF_3SO_3$. Bulk PPO and the PPO–$NaCF_3SO_3$ complexes were investigated using ^{13}C, ^{19}F and ^{23}Na nuclear magnetic resonance spectroscopy. Spin-lattice relaxation time, T_1, measurements were made as a function of temperature. The T_1 minima are observed for the different nuclei at different temperatures and concentrations of complexed salt. The ^{13}C T_1 data are interpreted in terms of a Cole–Cole distribution of correlation times. Polymer motion is discussed in the context of the nuclei probed.

(Keywords: ion-conducting polymer; polymer–salt complex; ^{13}C n.m.r. spectroscopy; ^{23}Na n.m.r. spectroscopy; ^{19}F n.m.r. spectroscopy)

INTRODUCTION

Polymer electrolytes have been the focus of numerous investigations by physicists, chemists and engineers during the past 10 years[1,2]. Potential applications of solvent-free polymer electrolytes with high ionic conductivities include high energy density batteries, specific ion electrodes, fuel cells and electrochromic displays[3]. A fundamental understanding of the mechanisms of ion transport in polymers is required to develop new polymer electrolyte systems.

A variety of physical and spectroscopic techniques have been utilized in the quest for insight into these systems, including audio-frequency electrical conductivity[4], differential scanning calorimetry[4,5], thermo-mechanical analysis[4], dielectric relaxation[6], X-ray absorption[7], infra-red and Raman spectroscopy[8,9] and nuclear magnetic resonance (n.m.r.)[4,5,10-14]. Among these methods, n.m.r. has been particularly useful in the characterization of amorphous and solid polymer electrolytes. Nuclei amenable to n.m.r. investigation naturally include the polymer chain backbone ^{13}C or ^{29}Si atoms and attached protons, ^{1}H, as well as many of the nuclei of the salts incorporated into polymer–salt complexes: ^{7}Li, ^{23}Na and ^{19}F. Diffusion[15] and relaxation[13] mechanisms can be probed for each nucleus, yielding information about the polymer electrolyte on time-scales complementary to other spectroscopic methods.

Polyether and siloxane-based polymers complexed with inorganic salts demonstrate significant levels of ionic conduction[11,16-18]. Systems based on poly(ethylene oxide), PEO, poly(propylene oxide), PPO, and polyether block copolymers of poly(dimethylsiloxane), PDMS, complexed with low lattice energy salts have been widely investigated. Spectroscopic investigations of PEO are complicated by regions of crystallinity in the polymer[19]. The ionic conductivity of PPO complexes is slightly lower than that of comparable complexes of PEO or PDMS blends[20]; however, PPO can be obtained as a completely amorphous material[21]. This fact, combined with the relatively simple polymer backbone structure, renders the PPO salt systems ideal for fundamental investigations of conducting polymer systems. In this paper, we present results of ^{13}C, ^{19}F and ^{23}Na n.m.r. investigations of PPO complexed with varying amounts of sodium trifluoromethanesulphonate, $NaCF_3SO_3$. The low molecular weight PPO which was utilized is a viscous liquid at room temperature as are the polymer–salt complexes.

EXPERIMENTAL

A PPO liquid polymer (Dow Chemical Company) with an average molecular-weight of ~ 3000 was used in these studies. The polymer was dried under vacuum at elevated temperatures. Reagent grade $NaCF_3SO_3$ (Alpha Chemicals) was dried in a similar manner. The two components were mixed in appropriate amounts and a volume of spectroscopic grade acetone approximately equal to that of the polymer was added to lower the viscosity of the polymer–salt system, facilitating stirring and homogeneity. The samples were then heated to 80°C under vacuum with stirring for 12 h or more to remove the acetone and any residual water. Six PPO–$NaCF_3SO_3$ complexes were prepared in this manner with ether oxygen:sodium ion ratios of 80:1, 40:1, 20:1, 15:1, 10:1 and 7.5:1.

All n.m.r. measurements were performed on a Varian XL-300 spectrometer using a variable-angle spinning probe (Doty Scientific). Samples were loaded under nitrogen into Macor rotors which were then closed with

* To whom correspondence should be addressed

0032-3861/91/162939-08

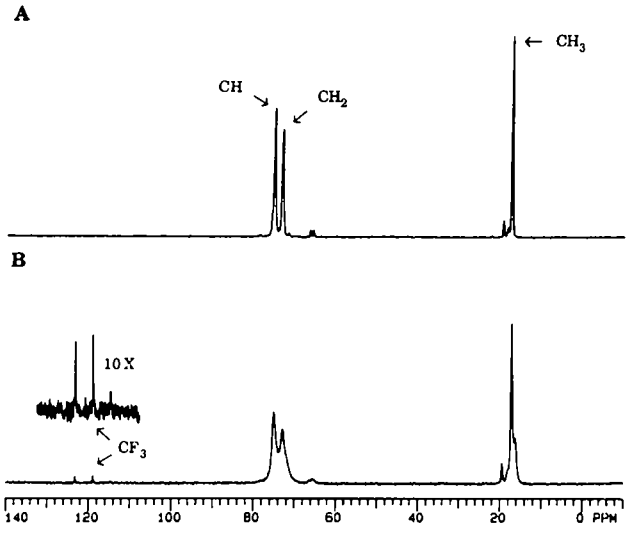

Figure 1 Proton decoupled ^{13}C n.m.r. spectra at 75.4 MHz and ambient temperature. (A)Bulk PPO and (B) the 20:1 PPO–$NaCF_3SO_3$ complex

a Teflon cap fitted with O-rings. The cap was sealed with a thin layer of epoxy. Samples were spun at the magic angle (54.7°). However, magic angle spinning is not a rigorous experimental requirement because the samples studied were viscous liquids rather than rigid solids. Sample temperatures were calibrated by observing ^1H signals of ethylene glycol on the carbon channel using the appropriate duty cycle. The temperature measurements are accurate to ± 1 K. The ^{13}C spin lattice relaxation data, T_1, were obtained at 75.4 MHz utilizing an inversion–recovery pulse sequence. The decoupler on-time duty cycle was $<3.5\%$. The ^{23}Na and ^{19}F T_1 data were obtained at 79.4 and 282.3 MHz, respectively, using a normal inversion–recovery pulse sequence. All T_1 data were processed on a VXR-4000 data station using the T_1 calculation programs provided by Varian.

RESULTS AND DISCUSSION

^{13}C n.m.r. spectra of PPO

A schematic diagram depicting the structure of PPO triol is given below:

$$\begin{array}{l} CH_2\text{-}\{OCH_2CH(CH_3)\}_{n_1}OH \\ | \\ CH\text{-}\{OCH_2CH(CH_3)\}_{n_2}OH \\ | \\ CH_2\text{-}\{OCH_2CH(CH_3)\}_{n_3}OH \end{array}$$

The PPO used in the present study was a polydisperse sample with an average molecular weight of ~3000. This molecular weight corresponds to an average of 50 repeat units ($n_1 + n_2 + n_3 \approx 50$) per polyether chain terminated with hydroxyl groups.

Room temperature ^{13}C n.m.r. spectra of bulk PPO and the 20:1 $NaCF_3SO_3$ complex are presented in *Figure 1*. The room temperature spectrum of PPO (*Figure 1A*) displays three bands at 17.6, 73.3 and 77.3 ppm, assigned to the methyl, methylene and methine carbons of the PPO chains, respectively. Smaller peaks, near the major bands, are attributed to carbons of the glycerine backbone and carbons of the PPO units at or near the end of the polymer chains, possessing somewhat different chemical shifts.

Upon complexation of PPO with $NaCF_3SO_3$ (*Figure 1B*), the band corresponding to the methyl carbon is split and a high-field shoulder appears. This new feature is first discernible in the spectrum of the 40:1 complex. It grows in intensity with increasing concentration of complexed salt and decreases in intensity in spectra acquired at higher temperature. Since atactic PPO was used in this work, differing orientations of the chiral centre (the methine carbon atom) along the polymer backbone result in inequivalent environments for the methyl groups. Random motions in the liquid polymer average these environments resulting in a single band for the methyl carbon in the spectrum of bulk PPO. In the polymer–salt complexes, interactions between oxygen atoms of the polymer backbone and a sodium cation form a local entity in which internal flexibility is greatly reduced, and the inequivalent environments become distinguishable. In other words, the formation of the local polymer–salt entity differentiates environments resulting from microtacticity of the polymer backbone, leading to the appearance of the high-field shoulder on the methyl resonance. It is also possible that similar changes occur for the methine and methylene signals; however, these bands are more severely broadened (*Figure 1B*) and splittings are not observed. The bandwidth of these features increases with increasing concentration of complexed salt and decreases with increasing temperature.

^{13}C T_1 studies of the methine and methylene carbon nuclei of the PPO backbone

^{13}C T_1s were measured as a function of temperature for the carbon atoms constituting the PPO backbone (the three major bands in *Figure 1*) in bulk PPO and each PPO–$NaCF_3SO_3$ complex. Although the partial overlap of the bands corresponding to the methine and methylene carbons made the calculation of T_1 values less accurate at lower temperatures and higher concentrations of complexed salt, the bands were sufficiently separated for T_1 to be well determined at all but the two lowest temperatures in the 10:1 complex and at the four lowest temperatures in the 7.5:1 complex. The results of these measurements are presented as data points in plots of $\ln T_1$ *versus* $1000/T$ for the methine carbon in *Figure 2* and the methylene carbon in *Figure 3*.

For motions on the time-scale observed in polymers, the ^{13}C relaxation is dominated by intramolecular dipole–dipole interactions with directly bonded protons. If one assumes a purely ^{13}C–^1H dipolar relaxation mechanism, T_1 observed in a ^{13}C experiment is given by the expression (in SI units)[22,23]:

$$T_1^{-1} = (\mu_0/4\pi)^2(h/2\pi)^2\gamma_C^2\gamma_H^2 \sum_i r_{C-H}^{-6}(1/10) \times [J_0(\omega_H - \omega_C) + 3J_1(\omega_C) + 6J_2(\omega_H + \omega_C)] \quad (1)$$

where $\mu_0/4\pi$ is the permeability constant, h is Planck's constant, γ_C and γ_H are the magnetogyric ratios of ^{13}C and ^1H, respectively, r_{C-H} is the bond distance separating the carbon atom from the ith proton (assumed to be 1.09 Å for all directly bonded C–H pairs) and the $J_n(\omega)$ are the spectral densities. The latter are calculated from the Fourier transforms of the normalized autocorrelation functions of the second-order spherical harmonics of the

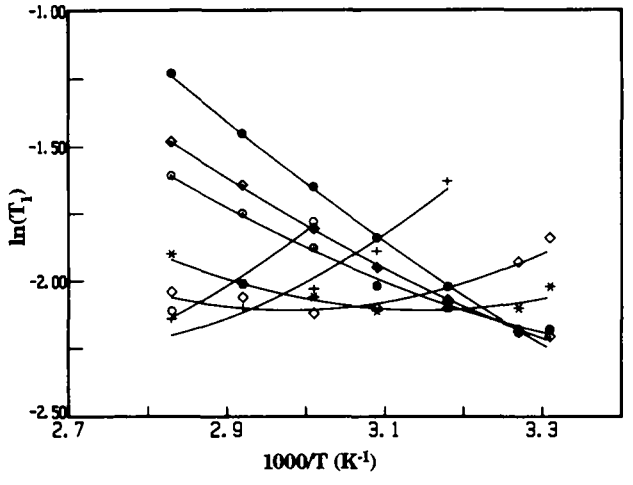

Figure 2 Ln T_1 *versus* $1000/T$ for the methine carbon in bulk PPO and PPO-$NaCF_3SO_3$ complexes. Experimental data points are labelled as follows: ●, bulk PPO; ◇, 80:1; ⊙, 40:1; *, 20:1; ⋄, 15:1; +, 10:1; ○, 7.5:1. The solid curves were calculated using equation (1) with spectral densities derived from a Cole–Cole distribution of correlation times and the parameters listed in *Table 1*

C–H bond orientation angles:

$$J_n(\omega) = 1/2 \int_{-\infty}^{\infty} f_n^2(\tau) f_n^2(0) \exp(i\omega\tau)\, d\tau \qquad (2)$$

For random, isotropic reorientation of the C–H internuclear vectors, the ensemble average of the autocorrelation functions is assumed to be well approximated by an exponential function with a single correlation time τ_c:

$$f_n^2(\tau) f_n^2(0) = \exp(-|\tau|/\tau_c) \qquad (3)$$

Explicit integration of equation (2) after substitution of equation (3) yields the familiar result:

$$J_n(\omega) = \tau_c/(1 + \omega^2\tau_c^2) \qquad (4)$$

The ratio $T_{1,CH}/T_{1,CH_2}$ observed at each temperature and concentration of complexed salt ranged from 1.4 to 1.6. These values differ considerably from the approximate value of 2 which would be expected from the number of directly bonded protons in the model described above. In addition, the values of the T_1 minima obtained were consistently higher than those predicted by this isotropic model. One reason for this is that the contribution to ^{13}C relaxation arising from non-bonded proton dipolar interactions is greater for the methine carbon than for the methylene carbon. Another reason is that the dynamics of C–H internuclear reorientation are not isotropic, and may be non-identical for the methine and methylene carbon atoms in the PPO backbone.

The connectivity of the polymer chain restricts the variety of motions available to a particular type of C–H internuclear vector and introduces a correlation between the orientation of these vectors in adjacent segments[24–26]. It has also been shown[27,28] that ^{13}C T_1 values of polymers in solution become independent of increasing chain length as the degree of polymerization approaches 100. These observations indicate that segmental or local motions, rather than the slow tumbling of the whole polymer chain, are responsible for spin-lattice relaxation in these polymers.

One model which correctly predicts the observed T_1 *versus* temperature behaviour incorporates a distribution of correlation times as described by Schaefer[29]. For a distribution of correlation times described by the normalized distribution function $G(\tau_c)$, the expression for the spectral densities given in equation (4) becomes:

$$J_n(\omega) = \int_0^{\infty} [G(\tau_c)\tau_c/(1 + \omega^2\tau_c^2)]\, d\tau_c \qquad (5)$$

Since n.m.r. correlation times span many orders of magnitude, it is convenient to define a new variable S:

$$S = \ln(\tau_c/\tau_0) \qquad (6)$$

where τ_0 is the mean correlation time about which the distribution function $G(\tau_c)$ is centred. The symmetric Cole–Cole[30,31] distribution function, used in the analysis of dielectric relaxation phenomena, has been previously applied to study ^{13}C spin-lattice relaxation in PPO[32]. We have found that it also provides excellent agreement with the experimental results presented in this work. The Cole–Cole distribution function of S, $L(S)$, is given by the expression[31]:

$$L(S) = (2\pi)^{-1} \sin(\gamma\pi)[\cosh(\gamma S) + \cos(\gamma\pi)]^{-1} \qquad (7)$$

The width parameter γ lies in the range 0–1 where $\gamma = 0$ represents an infinitely wide distribution and $\gamma = 1$ reduces to the situation of a single correlation time. *Figure 4* displays the form of the Cole–Cole distribution function for values of γ between 0.5 and 0.9. Using the relationship $G(\tau_c)\, d\tau_c = L(S)\, dS$, equation (5) may be explicitly integrated in the domain of S, yielding the expression for $J_n(\omega)$ under the influence of a Cole–Cole distribution of correlation times:

$$J_n(\omega) = (2\omega)^{-1} \cos[(1-\gamma)\pi/2] \times \{\cosh[\gamma \ln(\omega\tau_0)] + \sin[(1-\gamma)\pi/2]\}^{-1} \qquad (8)$$

In order to properly model the temperature dependence of the T_1 data, it was assumed that the mean correlation time τ_0 varies with temperature according to the Arrhenius equation:

$$\tau_0 = \tau_\infty \exp(E_a/RT) \qquad (9)$$

where τ_∞ is a highly empirical parameter corresponding

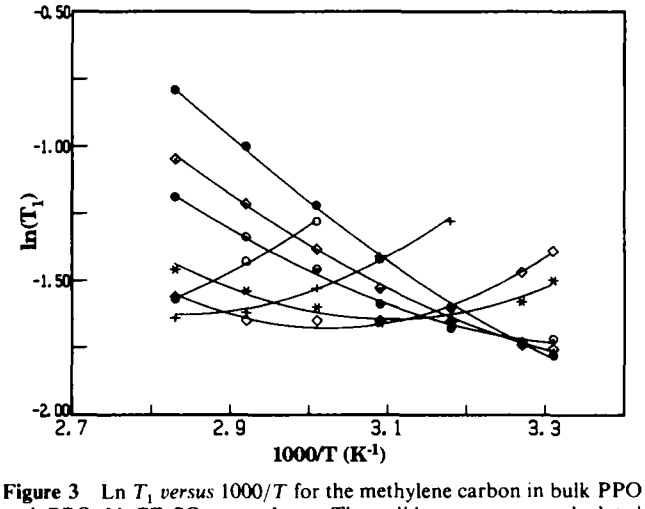

Figure 3 Ln T_1 *versus* $1000/T$ for the methylene carbon in bulk PPO and PPO-$NaCF_3SO_3$ complexes. The solid curves were calculated using equation (1) with spectral densities derived from a Cole–Cole distribution of correlation times and the parameters listed in *Table 1*. For symbols see *Figure 2*

to the value of the mean correlation time at the limit of infinitely high temperature and E_a is the apparent activation energy for the motions characterized by τ_0. The assumption that τ_0 varies with temperature in an Arrhenius-like manner in the temperature range under study is supported by other investigations applying independent models which describe the nature of the motions found in PPO[33] and other polymers[34].

The temperature dependence of the ^{13}C T_1 values for both the methine and methylene carbons was simultaneously determined by a non-linear least squares fit of the data using the distribution of correlation times model described above. In fitting the experimental data, it was found that only a single activation energy was necessary to describe T_1 values arising from both the methine and methylene carbons at a given concentration of complexed salt, whereas separate values of τ_∞ and the distribution width (γ) were required. The results are presented in *Table 1* and are plotted as solid curves through the data in *Figures 2* and *3*. As can be seen by the very close agreement between the calculated curves and experimental data, the temperature dependence of the ^{13}C T_1 values is well predicted assuming a Cole-Cole distribution of correlation times.

The data in *Table 1* show that E_a increases steadily with increasing concentration of complexed salt. The E_a of 23 kJ mol^{-1} calculated for bulk PPO compares quite favourably with values reported by Connor *et al.*[35] (28.5 kJ mol^{-1}) from ^1H T_1 measurements, Allen *et al.*[36] (18 kJ mol^{-1}) from incoherent neutron scattering, Jones and Wang[37] (25 kJ mol^{-1}) using Rayleigh scattering and Wang and Huang[38] (17 kJ mol^{-1}) using Brillouin scattering. However, higher values of the E_a have been reported from dielectric measurements by Baur and Stockmayer[39] (84 kJ mol^{-1}) and Yano *et al.*[40] (49 kJ mol^{-1}).

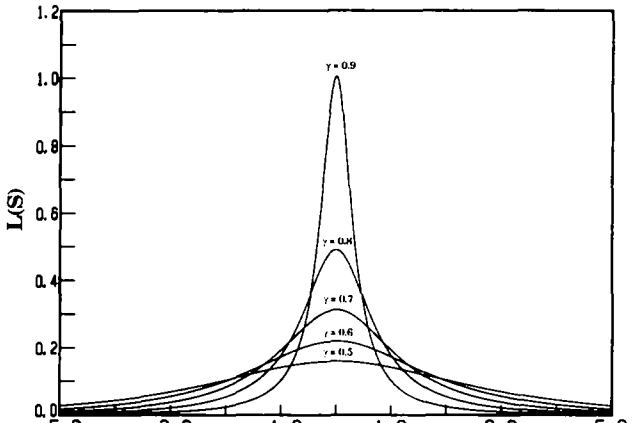

Figure 4 The form of the Cole-Cole distribution function for values of the width parameter, γ, ranging from 0.5 to 0.9

The data in *Table 1* demonstrate that τ_0 increases with increasing concentration at 332 K. Values of τ_0 behave similarly at each temperature studied. Increasing values of the mean correlation times for C–H internuclear reorientation indicate slower motions as more salt is complexed. Since the complexation process is thought to occur through coordination of the metal cation by ether oxygens and oxygens of the OH termini, it is likely that one metal cation can effectively bridge two or more polymer molecules through the formation of virtual crosslinks. The virtual crosslinks produce larger, more complex systems in which large scale segmental motion is hindered. With increasing concentration of complexed salt, the number of virtual crosslinks formed would increase and the configuration about each sodium ion would differ in the degree of intrachain (oxygens of a single polymer molecule complex a single metal cation) *versus* interchain (oxygens of two or more polymer molecules complex a single metal cation) complexation. Such a situation is compatible with the experimental observations presented.

The distribution width parameter (γ) shows a significant decrease upon introduction of the salt to PPO up to an ether oxygen:cation ratio of 40:1, and then remains more or less constant. This indicates that at lower concentrations of complexed salt, the polymer–salt interactions significantly alter the character of the motions which are responsible for relaxation of the ^{13}C nuclei of the polymer backbone. At higher concentrations of complexed salt, these motions become increasingly localized and the distribution widths for the two carbons demonstrate only very small changes.

^{13}C T_1 *studies of the methyl sidegroups on the PPO backbone*

^{13}C T_1s were measured as a function of temperature for the methyl groups on the PPO backbone in bulk PPO and each PPO–$NaCF_3SO_3$ complex. The results of these measurements are presented on a plot of ln T_1 *versus* 1000/T in *Figure 5*. The overall temperature dependence of the T_1 data for the methyl carbon is similar to that observed for the methine and methylene carbons. However, the presence of internal rotational freedom

Table 1 Results of least squares fits of ^{13}C T_1 data as a function of temperature for the methine and methylene carbon atoms of PPO using a Cole-Cole distribution of correlation times

Concentration	τ_∞ (CH,s)	τ_∞ (CH_2,s)	τ_0 (CH,s) at 332 K	E_a (kJ mol^{-1})	γ (CH)	γ (CH_2)
Bulk PPO	3.8×10^{-14}	2.5×10^{-14}	1.7×10^{-10}	23	1.0	0.92
80:1	1.7×10^{-15}	9.4×10^{-16}	2.0×10^{-10}	32	0.73	0.64
40:1	6.3×10^{-16}	3.2×10^{-16}	2.8×10^{-10}	36	0.66	0.56
20:1	3.5×10^{-17}	2.6×10^{-17}	8.1×10^{-10}	47	0.60	0.48
15:1	2.3×10^{-17}	2.9×10^{-17}	1.2×10^{-9}	49	0.62	0.48
10:1	3.4×10^{-17}	7.6×10^{-17}	3.6×10^{-9}	51[a]	0.59	0.54
7.5:1	2.2×10^{-17}	3.6×10^{-17}	9.7×10^{-9}	55[a]	0.58	0.56

[a]Those values which were not varied in the least squares calculations due to overlapping bands restricting the number of data points considered

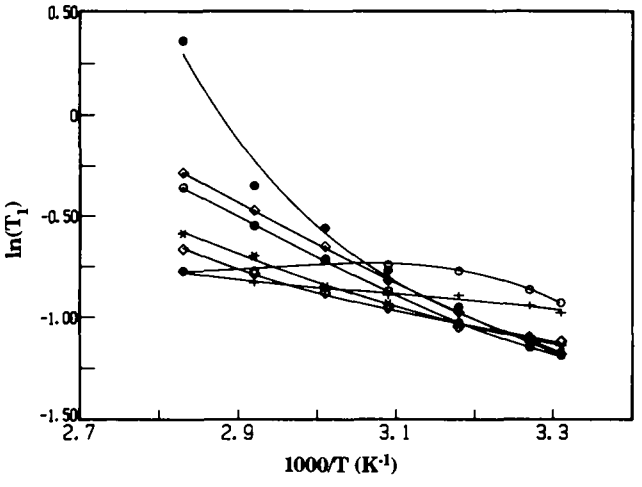

Figure 5 Ln T_1 *versus* 1000/T for the methyl carbon in bulk PPO and PPO-$NaCF_3SO_3$ complexes. The solid curves are empirical in nature and are only included to aid interpretation. For symbols see *Figure 2*

about the methyl three-fold axis complicates the interpretation of relaxation data.

In the temperature range under study, internal rotation and segmental motion are the motional processes which have the dominant effect on T_1. Since both processes are thermally activated, their major effect on T_1 will occur at different temperatures which depend upon the activation energies involved. The least energetic of these two processes is the internal rotation of the methyl group about its three-fold symmetry axis.

For bulk PPO at high temperature, the ratio $T_{1,CH}/T_{1,CH_3}$ approaches 1/3. In the absence of the internal rotation, consideration of the number of directly bonded protons should lead to an approximate value of 3 for this ratio; however, the internal rotation of the methyl group is extremely rapid in comparison to the other motional processes responsible for reorientation of the C–H internuclear vectors of the methyl group. When the diffusional correlation time describing rotation of the methyl group about its axis is much smaller than the isotropic correlation time τ_0, it may be shown[41] that the resulting anisotropy in the reorientational motion of the methyl C–H internuclear vectors reduces the effective correlation time by a factor of nine such that $\tau_{eff} = \tau_0/9$, and multiplication by the number of directly bonded protons in the limit of motional narrowing yields the observed ratio of 1/3.

At lower temperatures and increased concentrations of complexed salt the ratio $T_{1,CH}/T_{1,CH_3}$ increases. The influence of the internal rotation is most easily observed at high concentrations of complexed salt, since the activation energy for the segmental motion increases with concentration as shown in the analysis of the T_1 data for the methine and methylene carbons. This increase in activation energy forces the T_1 minimum associated with segmental motion to shift toward higher temperature, which falls beyond the range of our observation.

The turnover observed in the low temperature region of the curves for the 10:1 and 7.5:1 PPO-$NaCF_3SO_3$ complexes in *Figure 5* can be attributed to the increased relative contribution of the methyl rotation to relaxation of the methyl carbon. In fact, a small rise in T_1 occurring between two minima due to differing contributions of overall motion and internal rotation has been observed[35,42]. However, because of insufficient data due to the limitation in the temperature range of measurement, the experimental results could not be fitted to a model including internal rotation.

^{23}Na *spectra and* T_1 *studies*

Throughout the range of temperatures and concentrations of complexed salt studied, the band arising from the complexed sodium appeared as a single broad resonance. No evidence was found to support the existence of two bands corresponding to 'bound' (which has also been described as ion aggregates) and 'mobile' sodium ions which have been reported by Greenbaum and co-workers[4,11,43].

^{23}Na T_1s were measured as a function of temperature for the sodium nuclei in each PPO-$NaCF_3SO_3$ complex. The results of these measurements are presented on a plot of ln T_1 *versus* 1000/T in *Figure 6*. Temperature profiles for the 80:1 and 40:1 complexes display T_1 minima with shorter T_1 values for the 40:1 complex than those for the 80:1 complex. Temperature profiles for the 20:1, 15:1, 10:1 and 7.5:1 complexes display no T_1 minima and the T_1 values become consistently longer with increasing concentration of complexed salt. If one considers that T_1 minima move to higher temperature with increasing concentration of complexed salt, and that the minima appear at temperatures beyond the range of our measurement for the systems with higher concentrations of complexed salt, these observations can be readily understood.

^{23}Na is a quadrupolar nucleus with spin quantum number 3/2 and 100% natural abundance. Relaxation of the sodium cations is dominated by quadrupolar interactions with local electric field gradients. Quadrupolar relaxation is very efficient, causing T_1 values measured for ^{23}Na to be far smaller than those for ^{13}C or ^{19}F. T_1 data for each PPO-$NaCF_3SO_3$ complex were fitted to the expression:

$$T_1^{-1} = (3/10)\pi^2[(2I+3)/I^2(2I-1)]\chi^2[J_0(\omega_{Na})] \quad (10)$$

where I is the spin quantum number for ^{23}Na and is equal to 3/2, χ is the quadrupolar coupling constant for ^{23}Na in the PPO-$NaCF_3SO_3$ complex and $J_0(\omega_{Na})$ is

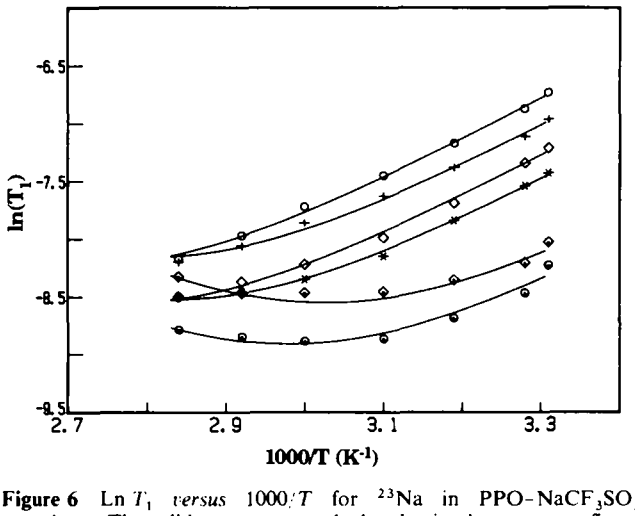

Figure 6 Ln T_1 *versus* 1000/T for ^{23}Na in PPO-$NaCF_3SO_3$ complexes. The solid curves were calculated using least squares fits of equation (10) with the parameters listed in *Table 2*. For symbols see *Figure 2*

Table 2 Results of least squares fits of ^{23}Na T_1 data as a function of temperature using equation (10) with $E_a = 30$ kJ mol^{-1}

Concentration	τ_∞ (s)	τ_0 (s) at 333 K	$\lvert\chi\rvert$ (MHz)
80:1	3.3×10^{-14}	1.8×10^{-9}	1.13
40:1	3.9×10^{-14}	2.2×10^{-9}	1.37
20:1	6.7×10^{-14}	3.7×10^{-9}	1.13
15:1	8.7×10^{-14}	4.8×10^{-9}	1.15
10:1	7.5×10^{-14}	4.1×10^{-9}	0.94
7.5:1	1.0×10^{-13}	5.7×10^{-9}	0.98

the spectral density for isotropic fluctuation of the local electric field gradients given by equation (4). The quadrupolar coupling constant, χ, is defined as $\chi = e^2Qq_{zz}/h$, where Q is the nuclear quadrupole moment for ^{23}Na, eq_{zz} is the local field gradient experienced by the ^{23}Na nucleus, e is the unit of elementary charge and h is Planck's constant. The temperature dependence of τ_c is assumed to follow the Arrhenius equation (equation (9)) over the small range of temperature under study.

The close agreement between the calculated curves and data points in *Figure 6* shows that equation (10) describes the experimental data quite well. In fitting the experimental data, it was found that a single E_a of 30 kJ mol^{-1} was sufficient to describe the temperature dependence of T_1 in all complexes but separate values of χ and τ_∞ were required for each system. Values of χ obtained from the least squares results ranged between 0.94 MHz and 1.37 MHz in magnitude without clear-cut trends.

The results of the least squares fits to equation (10) are presented in *Table 2*. τ_0 at 333 K increased with increasing concentration of complexed salt and values for low salt concentrations are larger than corresponding values for the polymer backbone (*Table 1*). This can be explained in the following manner. The correlation times of both the sodium ion and the methine and methylene segments are probably determined by motions of the local entity formed about the sodium ion upon complexation rather than rotational motions of the entire polymer. In addition, large scale segmental motions of the polymer backbone further reduce the mean correlation time of the methine and methylene groups at low salt concentration. As the number of virtual crosslinks grows with increasing concentration of complexed salt, the large scale segmental motions become more hindered. This would cause the mean lifetime of the sodium ion to approach those of the methine and methylene groups, as well as a change in χ. We must point out that there is most likely a small distribution of correlation times for the sodium ion, in spite of the fact that the experimental data can be well described using only a single correlation time in equation (10). This may explain the lack of a systematic trend in the calculated values of the χ (*Table 2*), the range of which appears to be quite reasonable when compared to those of sodium–crown ether complexes[44]. If a distribution of correlation times for the sodium ion were to be considered, results with more systematic changes might be obtained. However, we do not feel that it is advisable to introduce another variable parameter (γ) into the calculation without further justification.

^{19}F T_1 studies of fluorine nuclei in the trifluoromethanesulphonate anion

^{19}F T_1s were measured as a function of temperature for the trifluoromethanesulphonate anion in each PPO–$NaCF_3SO_3$ complex. The results of these measurements are presented as a plot of ln T_1 *versus* $1000/T$ in *Figure 7*. The T_1 *versus* inverse temperature profiles presented in *Figure 7* are quite similar to those of the methylene carbon in the PPO backbone (*Figure 3*). Over the range of temperature under study, T_1 values for the 80:1 complex display Arrhenius-like behaviour (ln T_1 *versus* $1000/T$ is linear) as would be expected for isotropic motion in the motional narrowing regime. However, with increasing concentration of complexed salt, correlation times for reorientational motion of the anion decrease and T_1 minima are observed. Judging from the T_1 data, the range of correlation times for the anion seems quite broad and similar to that displayed by the carbons of the PPO backbone, instead of behaving like a typical small ion in an isotropic medium. It is likely that motions of the anion are correlated to motions of the polymer due to ion pairing between the anions and polymer-complexed cations in highly concentrated systems.

^{19}F has a large magnetogyric ratio and its relaxation is determined by homonuclear dipolar interactions with neighbouring fluorine nuclei of the trifluoromethane group as well as the chemical shift anisotropy of each ^{19}F nucleus. The trifluoromethanesulphonate anion also possesses cylindrical symmetry and internal rotational freedom of the trifluoromethane group, making overall reorientational motion of the F–F internuclear vectors highly anisotropic. Because of this complication and the lack of detailed knowledge of the chemical shift anisotropy, the ^{19}F T_1 data were not fitted theoretically.

CONCLUSIONS

The present study of n.m.r. relaxation times has demonstrated the influence of polyether–salt interactions on local segmental motions of the polymer chain. The temperature dependence of the ^{13}C T_1 data for the methine and methylene carbons of the PPO backbone is well described by applying a Cole–Cole distribution of correlation times. To summarize our results and present an overall view of this investigation, T_1 curves calculated for the methine carbon as functions of τ_0 are shown in *Figure 8*. The three curves correspond to distribution

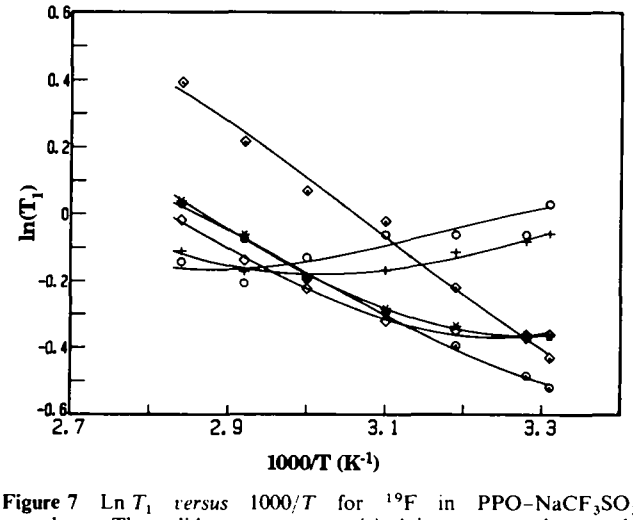

Figure 7 Ln T_1 *versus* $1000/T$ for ^{19}F in PPO–$NaCF_3SO_3$ complexes. The solid curves are empirical in nature and are only included to aid interpretation. For symbols see *Figure 2*

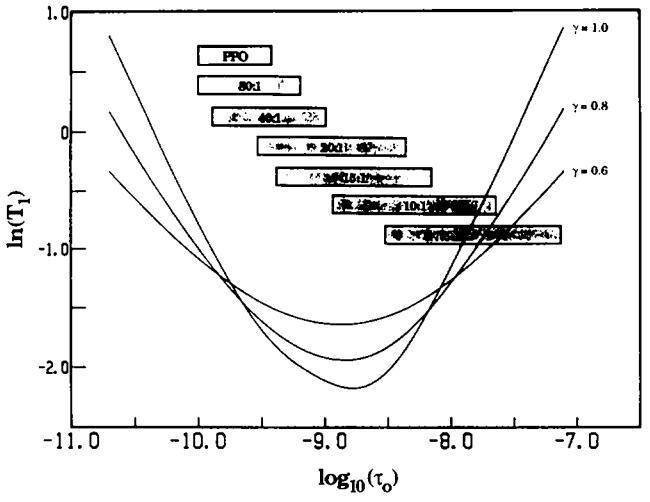

Figure 8 Ln T_1 *versus* $\log_{10} \tau_0$ for the methine carbon assuming a Cole–Cole distribution of correlation times with width parameter, γ, equal to 1.0, 0.8 and 0.6. Each shaded bar represents the range of correlation times determined by fitting the temperature dependence of the T_1 values for that PPO–$NaCF_3SO_3$ system. The left-hand border of each shaded bar corresponds to τ_0 at 353 K, and the right-hand border to τ_0 at 302 K. The detailed parameters derived from the least squares fits are listed in *Table 1*

width parameters (γ) of 1.0, 0.8 and 0.6, where $\gamma \approx 1.0$ reduces to the case of a single correlation time. The results of our least squares fits of T_1 as a function of temperature (*Table 1*) show that $\gamma = 1.0$ for uncomplexed PPO, $\gamma \approx 0.8$ for the 80:1 PPO–$NaCF_3SO_3$ complex and $\gamma \approx 0.6$ for the other polymer salt ratios (40:1, 20:1, 15:1, 10:1, 7.5:1) studied. The shaded bars represent the range of correlation times encountered in each PPO–$NaCF_3SO_3$ system between 353 K and 302 K. Extending each shaded bar vertically to the corresponding curve yields the region of experimentally determined T_1 values for that PPO–$NaCF_3SO_3$ system. Thus, it is quite clear why T_1 decreases with decreasing temperature for uncomplexed PPO and for complexes with larger polymer:salt ratios but increases with decreasing temperature for complexes with smaller polymer:salt ratios (*Figure 2*). It is important to note that almost three orders of magnitude of change in τ_0 are observed in these PPO–$NaCF_3SO_3$ systems. Increasing the salt concentration to create more virtual crosslinking causes τ_0 to increase rapidly, forcing the system to go through the T_1 minimum over a very narrow temperature range (51 K). This unusual behaviour has not been observed in many other systems. It demonstrates the success of the model with a distribution of correlation times applied to the Bloembergen, Purcell and Pound relaxation theory in a polymer system. The ^{13}C relaxation data for the methyl carbon of PPO are complicated by the presence of internal rotational freedom about its three-fold symmetry axis but are consistent with the segmental nature of the reorientational motion of the PPO backbone.

The χ and E_a for reorientational motion of the local electric field gradients experienced by the sodium cations were extracted by fitting the temperature dependence of the ^{23}Na T_1 data. The results substantiate the formation of Na^+–PPO complexes with increasing virtual crosslinking at higher concentrations of complexed salt.

^{19}F T_1 data were also collected as a function of temperature for the fluorine nuclei of the trifluoromethanesulphonate anion in the PPO–$NaCF_3SO_3$ complexes. The ^{19}F T_1 data indicate a broad range of reorientational motion for the anion, which may result from correlated motions of the anion and polymer originating from ion pairing between the anions and polymer-complexed cations. This conclusion is supported by vibrational spectroscopic studies of the PPO–$NaCF_3SO_3$ complexes which indicate that the anion is involved in a great deal of cation–anion association, particularly at higher concentrations of complexed salt[45-47]. In fact, recent studies in our laboratory suggest weak interactions exist between the cation and the CF_3 end of the anion throughout the range of concentrations studied[48].

ACKNOWLEDGEMENT

This work was supported by the US Department of Energy under grant no. DE-FG01-87FE61146.

REFERENCES

1 Armand, M. B. *Ann. Rev. Mater. Sci.* 1986, **16**, 245
2 MacCallum, J. R. and Vincent, C. A. (Eds) 'Polymer Electrolyte Reviews', Elsevier, London, 1987
3 Subbarao, E. C. (Ed.) 'Solid Electrolytes and Their Applications', Plenum, New York, 1980
4 Wintersgill, M. C., Fontanella, J. J., Smith, M. K., Greenbaum, S. G., Adamič, K. J. and Andeen, C. G. *Polymer* 1987, **28**, 633
5 Berthier, C., Gorecki, W., Minier, M., Armand, M. B., Chabagno, J. M. and Rigaud, P. *Solid State Ionics* 1983, **11**, 91
6 Fontanella, J. J. and Wintersgill, M. C. Office of Naval Research Technical Report No. 28, 1 July 1987
7 Den Boer, M. L. and Greenbaum, S. G. *Mol. Cryst. Liq. Cryst.* 1988, **160**, 339
8 Frech, R., Manning, J., Teeters, D. and Black, B. *Solid State Ionics* 1988, **28/30**, 954
9 Frech, R., Manning, J. and Black, B. *Polymer* 1989, **60**, 1785
10 Greenbaum, S. G. *Solid State Ionics* 1985, **15**, 259
11 Adamič, K. J., Greenbaum, S. G., Wintersgill, M. C. and Fontanella, J. J. *J. Appl. Phys.* 1986, **60**, 1342
12 Greenbaum, S. G., Pak, Y. S., Adamič, K. J., Wintersgill, M. C., Fontanella, J. J., Beam, D. A., Mei, H. L. and Okamoto, Y. *Mol. Cryst. Liq. Cryst.* 1988, **160**, 347
13 Spindler, R. and Shriver, D. F. *J. Am. Chem. Soc.* 1988, **110**, 3036
14 Komoroski, R. A. (Ed.) 'High Resolution NMR Spectroscopy of Synthetic Polymers in Bulk', VCH, Deerfield Beach, 1986
15 Bhattacharja, S., Smoot, S. W. and Whitmore, D. H. *Solid State Ionics* 1986, **18/19**, 306
16 Armand, M. B., Chabagno, J. M. and Duclot, M. J. in 'Fast Ion Transport in Solids' (Eds P. Vashishta, J. N. Mundy and G. K. Shenoy), Elsevier, New York, 1979, p. 131
17 Shriver, D. F., Papke, B. L., Ratner, M. A., Dupon, R., Wong, T. and Brodwin, M. *Solid State Ionics* 1981, **5**, 83
18 Weston, J. E. and Steele, B. C. H. *Solid State Ionics* 1982, **7**, 81
19 Weston, J. E. and Steele, B. C. H. *Solid State Ionics* 1981, **2**, 347
20 Watanabe, M., Nagano, S., Sanui, K. and Ogata, N. *Solid State Ionics* 1986, **18/19**, 338
21 Armand, M. *Solid State Ionics* 1983, **9/10**, 745
22 Allerhand, A., Doddrell, D. and Komoroski, R. *J. Chem. Phys.* 1971, **55**, 189
23 Schaefer, J. and Natusch, D. F. S. *Macromolecules* 1972, **5**, 416
24 Hermann, G. and Weill, G. *Macromolecules* 1975, **8**, 171
25 Hall, C. K. and Helfand, E. *J. Chem. Phys.* 1982, **77**, 3275
26 Viovy, J. L., Monnerie, L. and Brochon, J. C. *Macromolecules* 1983, **16**, 1845
27 Allerhand, A. and Hailstone, R. K. *J. Chem. Phys.* 1972, **56**, 3718
28 Chachaty, C., Forchioni, A. and Ronfard-Haret, J. C. *Makromol. Chem.* 1973, **173**, 213
29 Schaefer, J. *Macromolecules* 1973, **6**, 882
30 Cole, K. S. and Cole, R. H. *J. Chem. Phys.* 1941, **9**, 341
31 Connor, T. M. *Trans. Faraday Soc.* 1964, **60**, 1574
32 Heatley, F. and Begum, A. *Polymer* 1976, **17**, 399
33 Dejean de la Batie, R., Lauprêtre, F. and Monnerie, L. *Macromolecules* 1988, **21**, 2052
34 Dejean de la Batie, R., Lauprêtre, F. and Monnerie, L. *Macromolecules* 1988, **21**, 2045

35 Connor, T. M., Blears, D. J. and Allen, G. *Trans. Faraday Soc.* 1965, **61**, 1097
36 Allen, G., Brier, P. N., Goodyear, G. and Higgins, J. S. *Faraday Symp. Chem. Soc.* 1972, **6**, 169
37 Jones, D. R. and Wang, C. H. *J. Chem. Phys.* 1976, **65**, 1835
38 Wang, C. H. and Huang, Y. Y. *J. Chem. Phys.* 1976, **64**, 4847
39 Baur, M. E. and Stockmayer, W. H. *J. Chem. Phys.* 1965, **43**, 4319
40 Yano, S., Rahalkar, R. R., Hunter, S. P., Wang, C. H. and Boyd, R. H. *J. Polym. Sci., Polym. Phys. Edn* 1976, **14**, 1877
41 Harris, R. K. 'Nuclear Magnetic Resonance Spectroscopy. A Physicochemical View', Pitman, London, 1983, p. 115
42 Fleming, W. W., Lyerla, J. R. and Yannoni, C. S. in 'NMR and Macromolecules: Sequence, Dynamic and Domain Structure', American Chemical Society, Washington, 1984, p. 93
43 Greenbaum, S. G., Pak, Y. S., Wintersgill, M. C., Fontanella, J. J., Schultz, J. W. and Andeen, C. G. *J. Electrochem. Soc.* 1988, **135**, 235
44 Bisnaire, M., Detellier, C. and Nadon, D. *Can. J. Chem.* 1982, **60**, 3071
45 Schantz, S., Sandahl, J., Börjesson, L., Torell, L. M. and Stevens, J. R. *Solid State Ionics* 1988, **28/30**, 1047
46 Torell, L. M. and Schantz, S. 'Polymer Electrolyte Reviews 2' (Eds J. R. MacCallum and C. A. Vincent), Elsevier, London, 1989
47 Kakihana, M., Schantz, S. and Torell, L. M. *J. Chem. Phys.* 1990, **92**, 6271
48 Manning, J. P. and Frech, R. E. *Polymer* submitted